



Characterization of immune landscape and prognostic value of IL-17-related signature in invasive breast cancer

Wenge Dong[#], Xiaojie Gu[#], Jiejing Li[#], Zhigang Zhuang

Department of Breast Surgery, Shanghai Key Laboratory of Maternal Fetal Medicine, Shanghai Institute of Maternal-Fetal Medicine and Gynecologic Oncology, Shanghai First Maternity and Infant Hospital, School of Medicine, Tongji University, Shanghai, China

Contributions: (I) Conception and design: W Dong; (II) Administrative support: Z Zhuang; (III) Provision of study materials or patients: J Li; (IV) Collection and assembly of data: X Gu; (V) Data analysis and interpretation: Z Zhuang, J Li, X Gu; (VI) Manuscript writing: All authors; (VII) Final approval of manuscript: All authors.

[#]These authors contributed equally to this work.

Correspondence to: Zhigang Zhuang, MD. Department of Breast Surgery, Shanghai Key Laboratory of Maternal Fetal Medicine, Shanghai Institute of Maternal-Fetal Medicine and Gynecologic Oncology, Shanghai First Maternity and Infant Hospital, School of Medicine, Tongji University, 550 Hunan Road, Pudong New Area, Shanghai 201204, China. Email: Zhuang_zg@163.com.

Background: Recently, interleukin 17 (IL-17) has been found to play a critical role in the development of breast cancer. However, its prognostic significance in invasive breast cancer (IBC) remains unclear. This study aims to determine the role of IL-17-related signatures in IBC to identify novel therapeutic options.

Methods: IBC data from The Cancer Genome Atlas (TCGA), Gene Expression Omnibus (GEO), and Molecular Taxonomy of Breast Cancer International Consortium (METABRIC) were used to identify IL-17-related prognostic genes. A predictive model was developed using TCGA data and validated using METABRIC data. The relationship between IL-17 scores and immune landscape, chemotherapy drug sensitivity [half maximal inhibitory concentration (IC₅₀)], and immune checkpoint gene expression was analyzed. The quantitative reverse transcription polymerase chain reaction (qRT-PCR) was performed to validate key gene expression in breast tumor and normal tissue samples.

Results: The predictive model identified core IL-17-related prognostic genes and successfully estimated the prognosis of IBC patients. The model's validity was confirmed using METABRIC data. Patients with high IL-17 scores had worse overall survival (OS) compared to those with low IL-17 scores. Low IL-17 scores were associated with higher immune checkpoint gene expression and predicted enhanced responses to cytotoxic T-lymphocyte-associated protein 4 (CTLA4) and programmed cell death protein 1 (PD-1) therapies. Patients with low IL-17 scores exhibited a higher abundance of immune microenvironment components. Furthermore, qRT-PCR confirmed the lower expression of *OR51E1*, *NDRG2*, *RGS2*, and *TSPAN7* in breast tumors compared to normal tissue.

Conclusions: IL-17-related signatures are promising biomarkers for predicting the prognosis of IBC patients. These findings suggest that IL-17-related markers could be used to guide individualized therapeutic strategies, potentially improving outcomes for IBC patients.

Keywords: Interleukin 17 (IL-17); invasive breast cancer (IBC); immune microenvironment; prognostic biomarkers

Submitted Sep 05, 2024. Accepted for publication Jan 03, 2025. Published online Feb 26, 2025.

doi: 10.21037/tcr-24-1632

View this article at: <https://dx.doi.org/10.21037/tcr-24-1632>

Introduction

Breast cancer is a major global health challenge (1) and is one of the most common cancers in the world, with 2.26 million cases reported in 2020. Breast cancer is also the leading cause of cancer-related deaths among women (2). Invasive breast cancer (IBC) is the most common type of breast cancer worldwide. Despite advancements in the prognosis of the majority of patients with IBC, there remains a subset of patients with a dismal prognosis attributed to the inter-individual heterogeneity in tumor biology and prognostic outcomes (3). Therefore, novel biomarkers must be identified for patients with IBC.

Interleukin 17 (IL-17), a cytokine generated by CD8⁺ cells, $\gamma\delta$ T cells, NKT cells, ILC3s, and Th17 cells, is commonly increased in human inflammatory and autoimmune diseases (4). Owing to the discovery of the IL-23-Th17 immune axis, IL-17 is suggested to be linked to the progression of malignancy. This speculation has been verified by the discovery of increased IL-17 signature genes in several malignancies, including hepatocellular carcinoma, cervical cancer, gastric cancer, esophageal cancer, and colorectal cancer (5,6). Recently, IL-17 and IL-17-producing cells have been found to be increased in breast cancer (7,8), and numerous studies have found that IL-17 is associated with the development of breast cancer (9-12). For instance, Wu *et al.* demonstrated that the IL-17-CXC chemokine receptor 2 axis promotes breast cancer progression by upregulating neutrophil recruitment (9). Qian *et al.* found that an increased number of IL-17⁺ cells

in breast tumors predicts a poor prognosis for triple-negative breast cancer (TNBC) (10). IL-17 accelerates cell migration, enhances anoikis resistance, and creates an environment conducive to TNBC tumor metastasis (11). Furthermore, a previous study has indicated that increased numbers of IL-17-producing cells in the tumor microenvironment (TME) are associated with breast cancer subtypes exhibiting a higher degree of malignancy and short disease-free survival (12).

Interestingly, previous research has also revealed the dual role of Th17/IL-17 in tumor growth (13). On one hand, Th17 cells can contribute to tumor elimination by recruiting immune cells and promoting tumor cell death, thereby reducing tumor growth. On the other hand, Th17 cells can promote tumor growth through neo-angiogenesis, which involves the formation of new blood vessels. Th17 cells release factors that facilitate blood vessel development, providing oxygen and nutrients to the tumor and facilitating its growth and progression. The balance between these two roles depends on the specific TME and immune response, ultimately influencing overall tumor outcomes. These findings suggest that Th17/IL-17 may play an important role in the tumor immune microenvironment and impact tumor progression. However, the prognostic value and the immune microenvironment in IBC based on IL-17-related signatures remain unclear.

This study aimed to identify novel biomarkers for the generation of individualized therapies for patients with IBC. Using data from The Cancer Genome Atlas (TCGA) and the Molecular Taxonomy of Breast Cancer International Consortium (METABRIC) database, the function of the IL-17-related signature in IBC was assessed and validated. Based on core IL-17-related genes, a model for IBC prognosis was developed to predict the prognosis of IBC patients. Furthermore, to improve the utility and applicability of the IL-17-related signatures in clinical settings, the IL-17 score was integrated with clinicopathological prognostic factors to create a nomogram for more accurate clinical prognosis prediction. The immune infiltration characteristics of the TME, chemotherapy sensitivity, and immunotherapeutic response of IBC individuals with diverse IL-17 scores were analyzed to further explore the significance of the IL-17-related signature in the treatment of IBC. Such findings may be beneficial to the development of individualized breast cancer therapy. We present this article in accordance with the TRIPOD reporting checklist (available at <https://tcr.amegroups.com/article/view/10.21037/tcr-24-1632/rc>).

Highlight box

Key findings

- Interleukin 17 (IL-17)-related signatures are identified as promising biomarkers for predicting prognosis in invasive breast cancer (IBC).

What is known and what is new?

- Previous studies have highlighted IL-17's role in breast cancer development, but its prognostic significance in IBC is unknown.
- IL-17-related biomarkers could be integrated into clinical practice for predicting patient outcomes and tailoring individualized treatment strategies.

What is the implication, and what should change now?

- IL-17-related biomarkers could guide individualized therapeutic strategies in IBC, potentially leading to improved patient outcomes and more targeted treatment approaches.

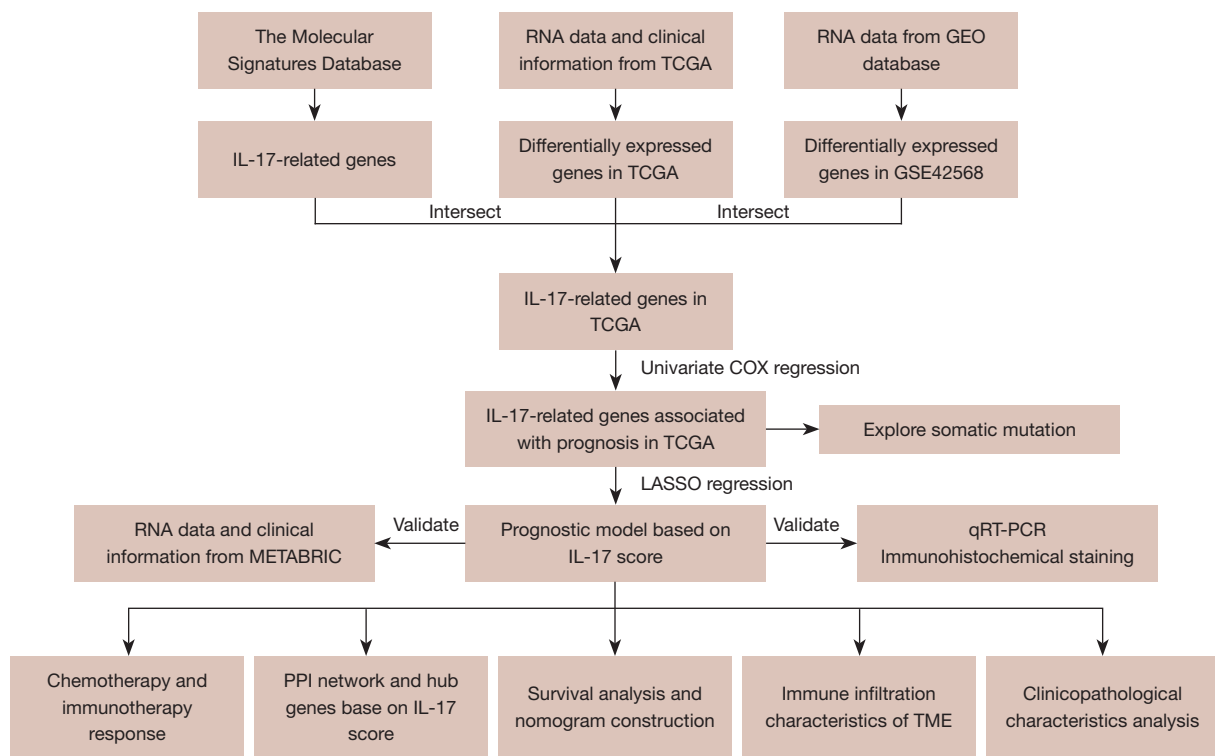


Figure 1 Flow chart. TCGA, The Cancer Genome Atlas; GEO, Gene Expression Omnibus; IL-17, interleukin 17; LASSO, least absolute shrinkage and selection operator; METABRIC, Molecular Taxonomy of Breast Cancer International Consortium; qRT-PCR, quantitative reverse transcription polymerase chain reaction; PPI, protein-protein network; TME, tumor microenvironment.

Methods

Data acquisition and compilation

This study utilized primary data sourced from TCGA, including 1,109 IBC and 113 normal breast samples. IBC data from the Gene Expression Omnibus (GEO) database (GSE42568) (14) were utilized to assist in the screening of IL-17-related genes, and data from METABRIC (15) database were used for validation. Two gene sets related to IL-17 (GSE10240_CTRL_VS_IL17_STIM_PRIMARY_BRONCHIAL_EPITHELIAL_CELLS_DN and GSE10240_CTRL_VS_IL17_STIM_PRIMARY_BRONCHIAL_EPITHELIAL_CELLS_UP) were obtained from Molecular Signature Database v7.5.1 (MSigDB). The flowchart is illustrated in *Figure 1*. The study was conducted in accordance with the Declaration of Helsinki (as revised in 2013).

Acquisition of IL-17-related differentially expressed genes (DEGs) in IBC

The “DESeq2” package was utilized to identify DEGs

by comparing IBC samples with normal breast tissues in the TCGA dataset (16). The “GEO2R” tool was used to identify the DEGs between IBC and normal breast tissues in GSE42568 (17). The DEGs in TCGA were intersected with the DEGs in GSE42568 and two gene sets related to IL-17 to obtain the IL-17-related DEGs in TCGA. DEGs were defined by a \log_2 fold change exceeding 1 and an adjusted P value below 0.05.

Development and evaluation of the prognostic model

The RNA data of IL-17-related DEGs and clinical information of IBC from TCGA were combined according to the sample ID. To screen prognostic genes in TCGA, univariate COX regression analysis was performed using the “survival” package (18). The “glmnet” and “survival” packages were used to perform least absolute shrinkage and selection operator (LASSO) logistic regression analysis (ten-fold cross-validation) to further identify the IL-17-related core prognostic genes and construct a prognostic model based on the IL-17 score in TCGA (19). The IL-

17 score of each patient was computed using the following formula: *OR51E1* expression value × corresponding coef + *NDRG2* expression value × corresponding coef + *SQLE* expression value × corresponding coef + *RGS2* expression value × corresponding coef + *TSPAN7* expression value × corresponding coef. The Shapiro-Wilk normality test and Wilcoxon rank-sum test were used to perform a difference analysis between the two groups. Somatic mutations in IBC samples from TCGA were analyzed using cBioPortal, an online platform for TCGA data exploration (<https://www.cbioportal.org/>) (20). The “survminer” and “survival” packages were used to perform Kaplan-Meier (K-M) survival analysis (18). The “factoextra” and “FactoMineR” packages were used to perform principal component analysis (PCA) (21). RNA data from METABRIC were used to validate the prognostic model constructed based on TCGA data using the same methodology described above.

Correlation between the clinicopathological characteristics and IL-17 score

The Spearman method was applied for correlation analysis. The Shapiro-Wilk normality test, Levene’s test, one-way analysis of variance (ANOVA), and Tukey’s honestly significant difference (HSD) test were used for difference analysis.

Construction of the nomogram for predicting the prognosis of IBC

The “survival” package was used to perform univariate COX regression analysis (18). The “rms” and “survival” packages were used to construct the nomogram and perform calibration analysis (number of samples for each group calculated repeatedly was set to 300; the number of repetitions was set to 1,000) (18). The “timeROC” package was employed for receiver operating characteristic (ROC) analysis (18). The K-M “survival” package and *stdca.R* file were used to perform the decision curve analysis (DCA) (22).

Function enrichment analysis

Gene Set Enrichment Analysis (GSEA) was conducted using the GSEA software (<http://software.broadinstitute.org/gsea/index.jsp>) with the “c2.cp.kegg.v7.4.symbols.gmt” gene sets from the Molecular Signatures Database. Statistical significance was defined as a P value <0.05 and a false discovery rate (FDR) <0.25. Gene Ontology

(GO) and Kyoto Encyclopedia of Genes and Genomes (KEGG) enrichment analyses were carried out using the “clusterProfiler” package (23).

Immune infiltration characteristics of the TME

The “GSVA” and “GSEABase” packages were applied to analyze immune cell infiltration and enrich immune-related pathways (24,25). The marker genes of immune cells were obtained from Bindea *et al.* (25) and are listed in Table S1. The “estimate” package was used to compute the immune and stromal scores in the low and high IL-17 score groups (26). The Shapiro-Wilk normality test and Wilcoxon rank-sum test were used to perform a difference analysis between the two groups.

Immunotherapy response and chemotherapy sensitivity

Data for immunogenomic analysis were sourced from The Cancer Immunome Atlas (TCIA) website (<https://tcia.at/home>) (27). The Shapiro-Wilk normality test and Wilcoxon rank-sum test were used to perform a difference analysis between the two groups. The “oncopredict” package was used to perform drug sensitivity analysis (28). The Spearman method was used to perform correlation analysis.

Construction of the protein-protein interaction (PPI) network and identification of hub genes

Differential analysis was conducted using the “limma” package, which identified DEGs between the low and high IL-17 score groups (29). STRING (<https://cn.string-db.org/>) provided data for constructing the PPI network (30). The PPI network was visualized using Cytoscape software (31), with CytoHubba, a Cytoscape plug-in, used to identify hub genes (32). Node scores in CytoHubba were calculated to rank the top ten hub nodes based on the radiality method as hub genes.

Quantitative reverse transcription-polymerase chain reaction (qRT-PCR) and Immunohistochemical staining

RNA was extracted from 15 breast tumor and 12 adjacent normal breast tissues using Total RNA Extraction Reagent (Trizol) (Abclonal, Wuhan, China, RK30129) according to the manufacturer’s protocol. Reverse transcription utilized 1 µg of RNA and ABScript III RT Master Mix (Abclonal, RK20428). qRT-PCR analysis was conducted with

Genlous 2× SYBR Green PCR Fast qPCR Mix (Low ROX Premixed) (Abclonal, RK21206). Target gene mRNA levels were normalized to beta-actin using the $2^{-\Delta\Delta CT}$ method. Primer sequences are detailed in [Table S2](#).

Images of normal breast and tumor tissues following immunohistochemical staining were obtained from the Human Protein Atlas (HPA) database (<https://www.proteinatlas.org/>), a publicly available resource that comprises numerous immunohistochemical images of human tumors and normal tissues. The antibodies used for immunohistochemical staining were CAB019995 (OR51E), HPA002896 (NDRG2), HPA020762 (SQLE), and CAB068245 (TSPAN7).

Single cell analysis

TISCH (<http://tisch.comp-genomics.org>), an online tool for single-cell RNA-seq analysis of the TME, was applied to investigate cell type heterogeneity in the breast cancer TME.

Statistical analysis

Data analysis and visualization were performed using R software (version 3.6.3 and 4.2.1). Correlation analysis was conducted using the Spearman method. Difference analysis was carried out using the Shapiro-Wilk normality test, Levene's test, one-way ANOVA test, or Tukey's HSD test. Survival analysis was performed using the overall survival (OS) time of IBC patients. The median of the input variate was used as the cut-off value for K-M survival analysis, following the usual practice. The median OS time of the patients included in the analysis was 865 (range, 466, 1,690) days in TCGA cohort and was 3,209 (range, 1,643, 5,122) days in METABRIC cohort, respectively. Statistical significance was considered when the P value was less than 0.05.

Results

Identifying IL-17-related DEGs in IBC

First, differential gene analysis was performed using the genes in IBC and normal breast samples from TCGA and GEO (GSE42568) databases. As a result, 10,278 DEGs were identified in TCGA and 3,196 DEGs were identified in GSE42568. Thereafter, 44 IL-17-related DEGs were identified in TCGA by intersecting the DEGs in TCGA,

GSE42568, and 389 IL-17-related genes from MSigDB ([Figure 2A](#)).

Construction of a prognostic model based on the IL-17 score in IBC

By performing univariate COX regression analysis, five genes (*OR51E1*, *NDRG2*, *SQLE*, *RGS2*, and *TSPAN7*) associated with the prognosis of patients with IBC were screened out from the 44 IL-17-related DEGs ([Table 1](#)). These five genes were identified as core prognostic genes using LASSO regression analysis ([Figure 2B](#)). [Figure 2C](#) shows the difference in expression of the five core IL-17-related genes between normal breast tissues and IBC. Based on [Figure 2C](#), *OR51E1*, *NDRG2*, *RGS2*, and *TSPAN7* had lower expression in IBC tissues than in normal breast tissues, while *SQLE* had higher expression in IBC tissues than in normal breast tissues. Correlation analysis was performed to determine the correlation between the five genes.

In addition, we analyzed the expression levels of *OR51E1*, *NDRG2*, *SQLE*, *RGS2*, and *TSPAN7* across the TNBC, luminal, and HER2-enriched subtypes ([Figure 2D](#)). Our results revealed distinct expression patterns for each gene across these subtypes. Specifically, *OR51E1* expression was significantly higher in the HER2-enriched subtype compared to both TNBC and luminal ($P < 0.05$). *NDRG2* and *SQLE* showed notably elevated expression in TNBC relative to luminal ($P < 0.001$ for *NDRG2* and $P < 0.001$ for *SQLE*). Furthermore, *RGS2* expression was significantly higher in TNBC ($P < 0.001$), while *TSPAN7* expression was more pronounced in luminal ($P < 0.001$) compared to the other subtypes. These findings highlight the subtype-specific variability in IL-17-related gene expression, suggesting that IL-17 signaling pathways may contribute uniquely to the tumor biology of each breast cancer subtype.

To explore the mutations in the five core genes, the mutation data of IBC patients from cBioPortal were analyzed ([Figure 2E](#)). Mutation was identified in 282 (29%) of the 963 samples, and most alterations were amplified. In addition, *SQLE* had the highest mutation frequency (up to 20%). LASSO regression was then used to construct a prognostic prediction model based on the IL-17-related core genes in patients with IBC. The IL-17 score of each patient was computed using the following formula: *OR51E1* expression value \times (0.580110283) + *NDRG2* expression value \times (-0.085565983) + *SQLE* expression value \times

Table 1 Results of univariate COX regression of the 5 genes

Gene symbol	HR (95% CI)	P value
<i>OR51E1</i>	1.811 (1.128–2.908)	0.01
<i>NDRG2</i>	0.837 (0.718–0.975)	0.02
<i>SQLE</i>	1.194 (1.023–1.393)	0.03
<i>RGS2</i>	0.873 (0.768–0.992)	0.04
<i>TSPAN7</i>	0.834 (0.703–0.991)	0.04

HR, hazard ratio; CI, confidence interval.

Validation of the prognostic model based on IL-17 score in IBC

To validate the prognostic model based on the IL-17 score, IBC data from METABRIC were utilized to construct the prognostic model in the same manner as above. The analysis results revealed that patients with low IL-17 scores had better OS than those with high IL-17 scores [HR =1.48 (95% CI: 1.31–1.69); $P < 0.001$] (*Figure 3B*). In addition, the image depicting the survival status and the five core prognostic gene expression levels in the low and high IL-17 score groups and PCA revealed good discrimination between the two groups (*Figure 3B*), aligning with the results in TCGA. These results verified the excellent accuracy of the prognostic model based on the IL-17 score in TCGA.

Correlation between the IL-17 score and clinicopathological characteristics or indicators

To assess the relationship between IL-17 score and the clinicopathological characteristics or indicators of IBC patients, patients with different IL-17 scores were compared to analyze differences in age, T stage, N stage, pathological stage and subtype. As shown in *Figure 3C*, age was positively correlated with IL-17 score ($r = 0.065$; $P = 0.04$). In addition, patients with T4 stage disease had the highest IL-17 score, and patients with N3 stage disease had the lowest IL-17 score. However, there was no difference between the pathological stage and IL-17 score. Moreover, patients with HER2-enriched breast cancer had the highest IL-17 score, while patients with TNBC had the lowest IL-17 score among the breast cancer subtypes, including HER2-enriched, luminal, and TNBC. Furthermore, the IL-17 score demonstrated a positive correlation with the expression of the proliferation-associated gene *MKI67* ($r = 0.301$; $P < 0.001$), while it exhibited a negative correlation

with the ESTIMATE immune score ($r = -0.216$; $P < 0.001$). To further investigate the prognostic role of the IL-17 score in different subtypes of breast cancer, patients with different subtypes were divided into high and low IL-17 groups and included in the K-M survival analysis. As illustrated in *Figure 4A*, HER2-enriched [HR =0.20 (95% CI: 0.04–0.94); $P = 0.042$] and TNBC patients [HR =0.33 (95% CI: 0.12–0.89); $P = 0.03$] demonstrated a superior OS in the low IL-17 score group compared to the high IL-17 score group, which corroborated the results observed in IBC. However, no significant difference in OS was observed among luminal patients between the high and low score groups [HR =0.73 (95% CI: 0.36–1.46); $P = 0.37$]. In addition, the relationship between IL-17 scores and the tumor angiogenesis marker vascular endothelial growth factor (*VEGF*) was further investigated to explore the role of IL-17 scores in tumor angiogenesis. As shown in *Figure 4B*, the high IL-17 score group exhibited higher *VEGF* expression compared to the low IL-17 score group. Furthermore, K-M survival analysis revealed that patients with low *VEGF* expression had a better OS in the high IL-17 score group compared to the low IL-17 score group (*Figure 4B*) [HR =2.06 (95% CI: 1.27–3.36); $P = 0.004$]. Conversely, patients with high *VEGF* expression showed no significant difference in OS between the high IL-17 score group and the low IL-17 score group (*Figure 4B*) [HR =1.51 (95% CI: 0.95–2.40); $P = 0.08$].

Construction of the nomogram for predicting the prognosis of IBC

To further explore the correlation between prognosis and the IL-17 score and clinicopathological characteristics of IBC, the IL-17 score, age, T stage, N stage, and pathological stage and PAM50 subtype were included in the univariate and multivariate COX regression analyses to identify independent prognostic factors. As depicted in *Tables 2,3*, the IL-17 score (HR =2.65; $P < 0.001$), age (HR =1.04; $P < 0.001$), T stage (HR =1.83; $P = 0.002$), N stage (HR =2.25; $P < 0.001$), pathological stage (HR =2.53; $P < 0.001$), basal-like subtype (HR =0.44; $P = 0.003$), luminal A (HR =0.29; $P < 0.001$) and B (HR =0.46; $P = 0.006$) subtypes were prognostic factors based on univariate COX regression, while only age (HR =1.04; $P < 0.001$), pathological stage (HR =2.42; $P = 0.02$), luminal A (HR =0.28; $P < 0.001$) and B (HR =0.30; $P < 0.001$) subtypes, and IL-17 score (HR =2.60; $P = 0.001$) were independent prognostic factors. To enhance the clinical applicability and accuracy of the prediction model, age, pathological stage and IL-17 score

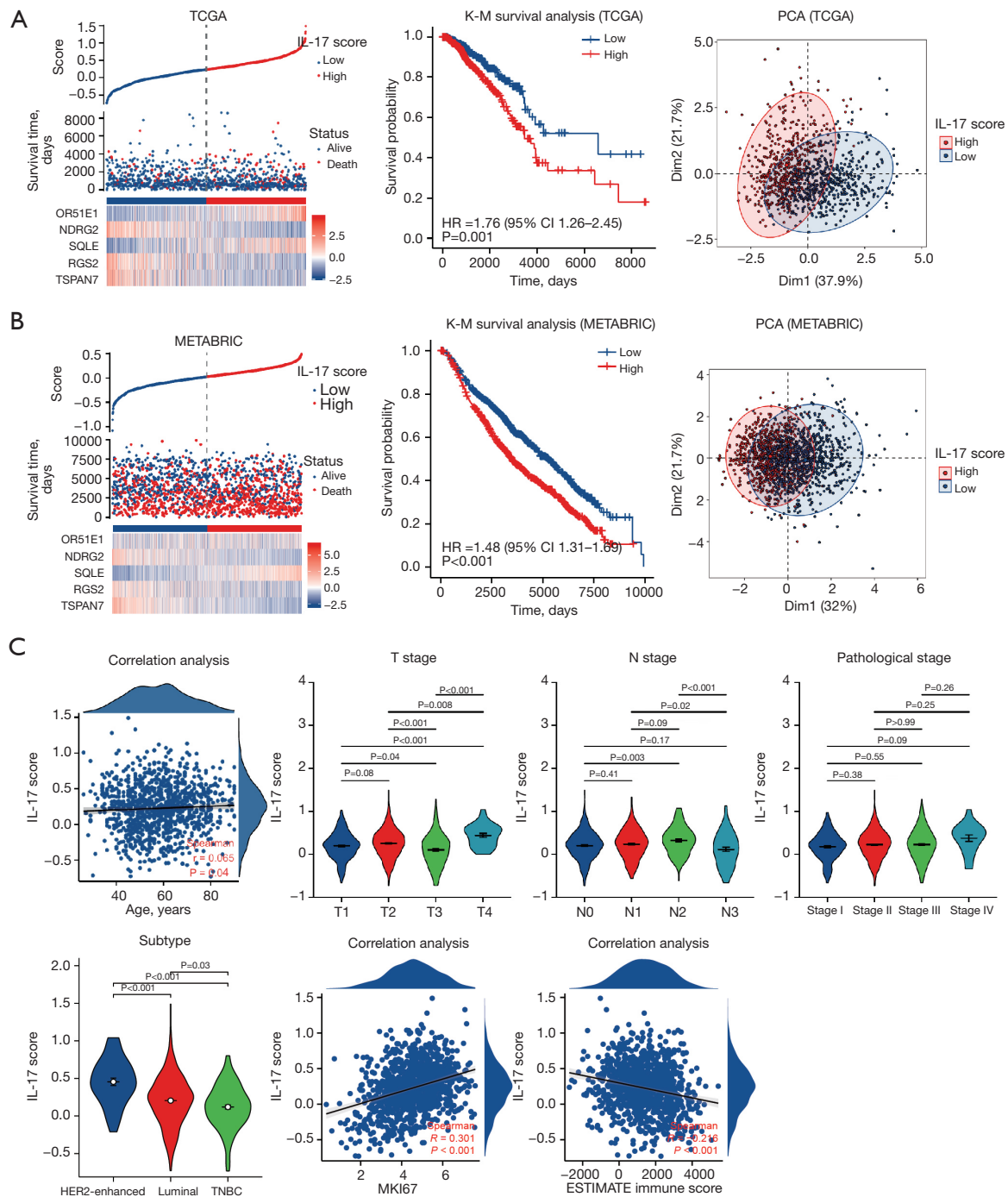


Figure 3 Construction and validation of the prognostic model based on IL-17 score. (A) The heat map combined with survival status, IL-17 score distribution, and expression difference in the 5 core prognostic genes, K-M survival curves of patients with low and high IL-17 score in TCGA, and PCA based on the 5 core prognostic genes in TCGA. (B) The heat map combined with survival status, IL-17 score distribution, and expression difference in the 5 core prognostic genes, K-M survival curves of patients with low and high IL-17 score in METABRIC, and PCA based on the 5 core prognostic genes in METABRIC. (C) The relationship between IL-17 scores and age, T stage, N stage, pathological stage, breast cancer subtypes, *MKI67* expression and ESTIMATE immune score, respectively. TCGA, The Cancer Genome Atlas; IL-17, interleukin 17; K-M, Kaplan-Meier; HR, hazard ratio; PCA, principal component analysis; METABRIC, Molecular Taxonomy of Breast Cancer International Consortium; HER2, human epidermal growth factor receptor 2; TNBC, triple-negative breast cancer.

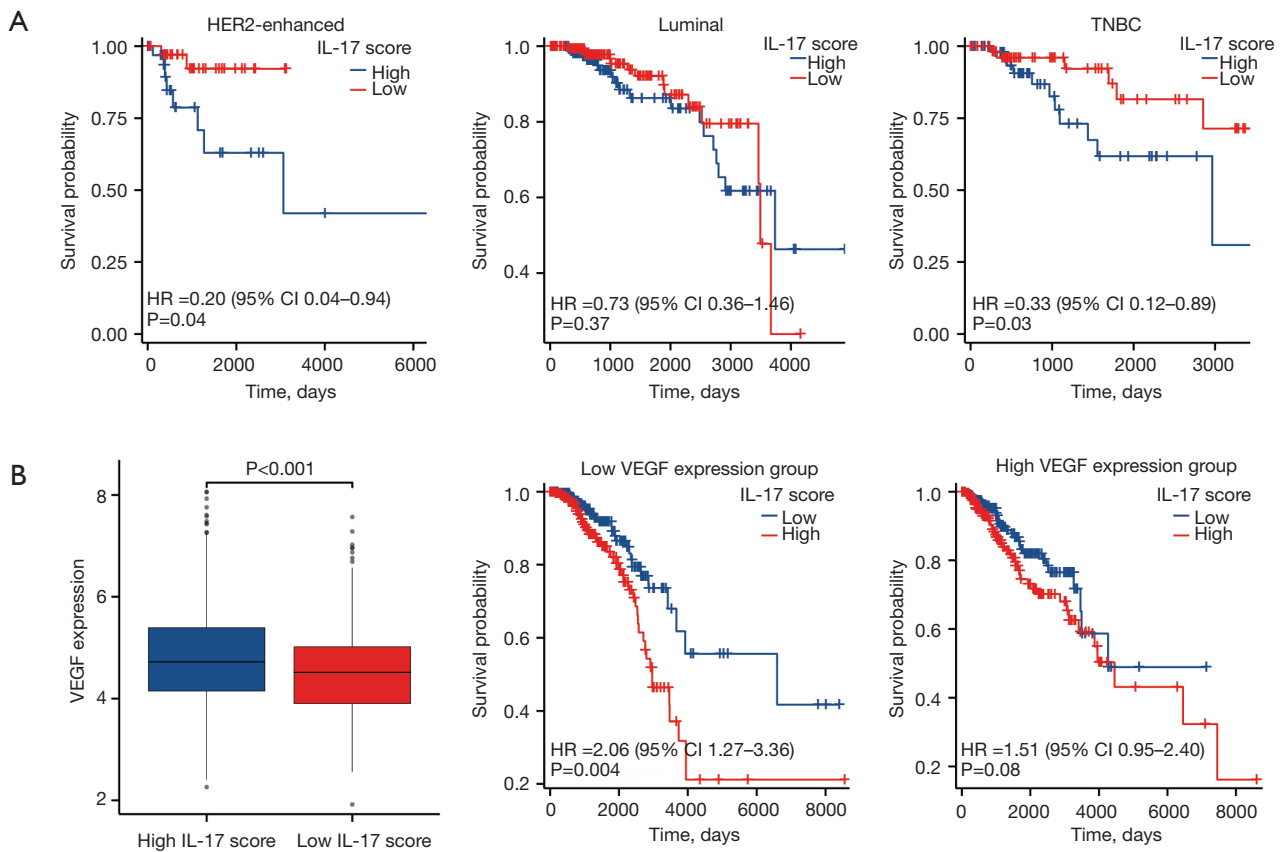


Figure 4 Further investigation of the relationship between IL-17 score, breast cancer subtypes, and *VEGF* respectively. (A) The results of Kaplan-Meier survival analysis for high and low IL-17 score groups within the context of different breast cancer subtypes. (B) Differential expression of *VEGF* between the low and high IL-17 score groups, and Kaplan-Meier survival analysis of IL-17 score in patients with low and high *VEGF* expression levels respectively. HER2, human epidermal growth factor receptor 2; IL-17, interleukin 17; HR, hazard ratio; TNBC, triple-negative breast cancer; *VEGF*, vascular endothelial growth factor.

Table 2 Results of univariate COX analysis of IL-17 score and clinicopathological features

Variate	HR	95% CI	P value
Age	1.035554343	1.021546553–1.049754213	<0.001
T (T1&T2 vs. T3&T4)	1.825103749	1.238628363–2.68926806	0.002
N (N0&N1 vs. N2&N3)	2.245568379	1.508381777–3.343037832	<0.001
Pathologic stage (I&II vs. III&IV)	2.534427313	1.785401904–3.597689568	<0.001
PAM50 (vs. subtype normal-like)			
Subtype basal-like	0.440716992	0.25684727–0.756213866	0.003
Subtype HER2-enhanced	0.612835342	0.306092254–1.226973736	0.17
Subtype luminal A	0.291957393	0.187944928–0.453532428	<0.001
Subtype luminal B	0.461075794	0.264499654–0.80374732	0.006
IL-17 score	2.650800823	1.542800718–4.554538326	<0.001

IL-17, interleukin 17; HR, hazard ratio; CI, confidence interval; HER2, human epidermal growth factor receptor 2.

Table 3 Results of multivariate COX analysis of IL-17 score and clinicopathological features

Variate	Coef	HR	95% CI of HR	P value
Age	0.036491212	1.037165189	1.023399727–1.051115806	<0.001
T (T1&T2 vs. T3&T4)	0.159216283	1.17259153	0.666888729–2.061769583	0.58
N (N0&N1 vs. N2&N3)	0.20027765	1.221741927	0.627046125–2.380452215	0.57
Pathologic stage (I&II vs. III&IV)	0.885347532	2.423826603	1.186478075–4.951575191	0.02
PAM50 (vs. subtype normal-like)				
Subtype basal-like	–0.503815598	0.604220792	0.348903105–1.046372934	0.08
Subtype HER2-enhanced	–0.687568133	0.50279732	0.241627813–1.046258466	0.07
Subtype luminal A	–1.268663206	0.281207287	0.179955171–0.439429095	<0.001
Subtype luminal B	–1.209177789	0.298442561	0.16612794–0.536140776	<0.001
IL-17 score	0.957270149	2.604576654	1.449897593–4.678826683	0.001

IL-17, interleukin 17; HR, hazard ratio; CI, confidence interval; HER2, human epidermal growth factor receptor 2.

were included to construct a nomogram for predicting the OS of patients with IBC (*Figure 5A*). The ROC curve was used to determine whether the predictive power of the nomogram was the best among the parameters including age, pathological stage, and IL-17 score. As shown in *Figure 5B*, the 1-, 3-, and 5-year area under the curve (AUC) values of the nomogram (0.869, 0.761, and 0.739) were larger than those of age (0.804, 0.638, and 0.638), pathological stage (0.717, 0.697, and 0.642), and IL-17 scores (0.594, 0.600, and 0.633), thereby illustrating the strong ability of the nomogram to predict the prognosis of IBC. The results of the 1-, 3-, and 5-year DCA suggested that the nomogram had the best clinical utility compared to other parameters (*Figure 5C*). In addition, the calibration plot showed that the nomogram for predicting the prognosis of patients had a good predictive ability (*Figure 5D*). Based on these results, the nomogram prediction model based on the IL-17 score and clinicopathological features has been verified from many aspects and has been proven to have a strong prediction ability and good clinical utility.

Function enrichment analysis

To examine the IL-17 signature-related biological function and pathways, GSEA, GO, and KEGG enrichment analyses were performed. The low and high IL-17 score groups were compared to identify the differential biological functions and pathways between the two groups. As shown in *Figure 6A, 6B*, arachidonic acid metabolism, FCepsilonRI

signaling pathway, ether lipid metabolism, JAK-STAT signaling pathway, and basal cell carcinoma were significantly enriched in the low IL-17 score group, whereas steroid biosynthesis, protein export, valine leucine and isoleucine biosynthesis, biosynthesis of unsaturated fatty acids, and terpenoid backbone biosynthesis were significantly enriched in the high IL-17 score group. The IL-17-related core genes were also included in the GO and KEGG enrichment analyses to identify possible biological functions and pathways. As shown in *Figure 6C*, the GO enrichment results include the regulation of amino acid transmembrane transport, relaxation of smooth muscle, negative regulation of the MAPK cascade, site of polarized growth, growth cone, cytoplasmic side of the plasma membrane, beta-tubulin binding, flavin adenine dinucleotide (FAD) binding, and G-protein alpha-subunit binding, while the KEGG enrichment results included oxytocin signaling pathway, olfactory transduction, and steroid biosynthesis.

Immune infiltration characteristics of the TME

Owing to mounting evidence that immune infiltration characteristics play a significant role in the development of breast cancer, the relationship between immune infiltration characteristics and IL-17 score was assessed. As shown in *Figure 7A*, most of the immune cells in the low IL-17 score group had significantly higher infiltration fractions, with the exception of Th2 cells. Further, *Figure 7B* shows that most immune-related pathways, such as checkpoints,

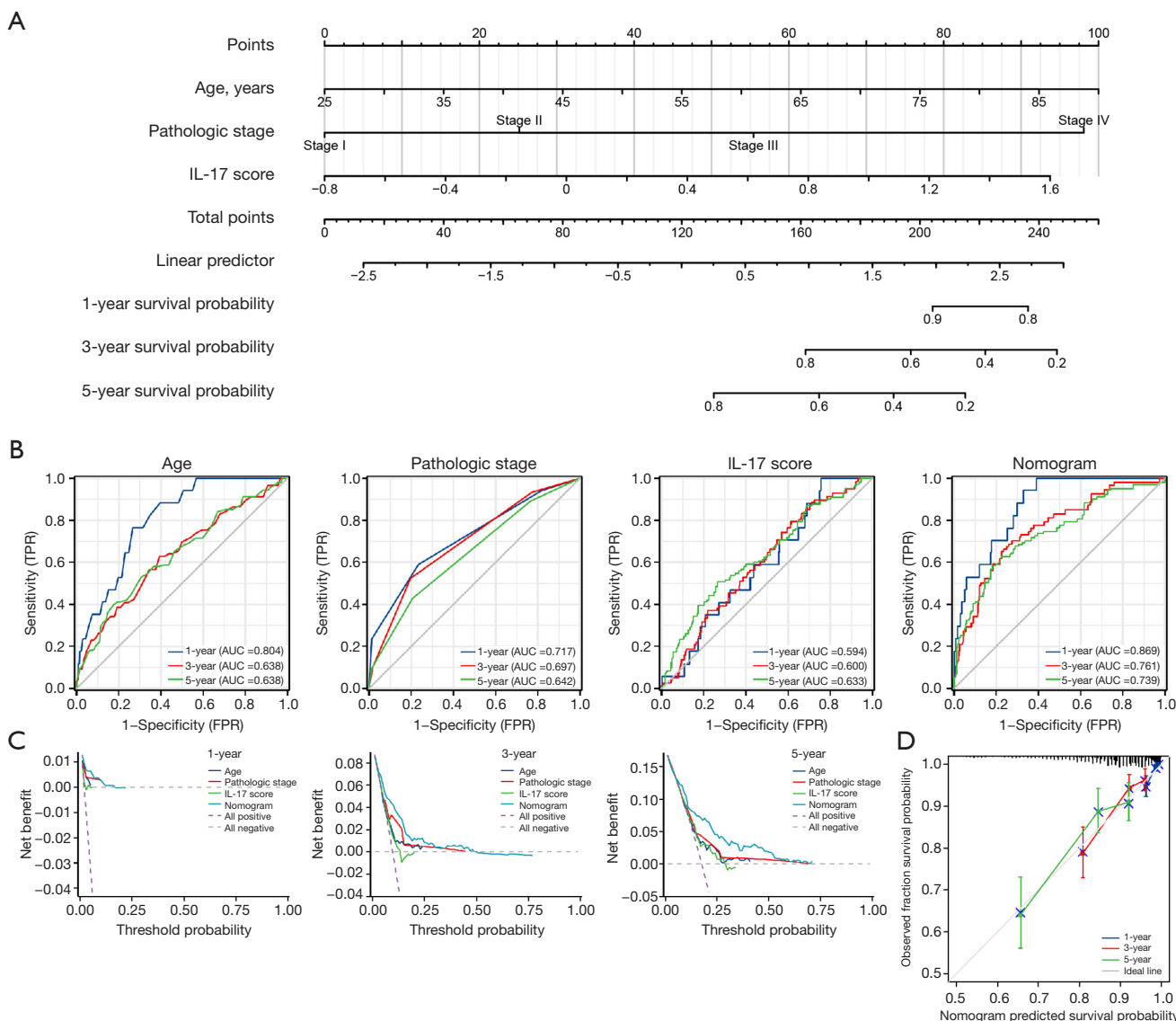


Figure 5 Development of a nomogram integrating IL-17 score and clinicopathological characteristics to predict OS in IBC patients, along with its accuracy validation. (A) Nomogram predicting 1-, 3-, and 5-year OS of IBC patients. (B) Time-independent ROC curves comparing the nomogram and independent prognostic indicators. (C) DCA evaluating nomogram accuracy. (D) Calibration plots of the nomogram. IL-17, interleukin 17; TPR, true positive rate; FPR, false positive rate; AUC, area under the curve; OS, overall survival; IBC, invasive breast cancer; ROC, receiver operating characteristic; DCA, decision curve analysis.

were highly enriched in the low IL-17 score group. The low IL-17 score group had a higher immune score and stromal score than the high IL-17 score group, as shown in *Figure 7C*. These results suggest that in the TME of IBC, immune microenvironment components are more enriched in patients with low IL-17 scores. Moreover, the role of IL-17 score in relation to immune infiltration cells in different breast cancer subtypes was further investigated. As

shown in *Figure 7D*, consistent with the results of immune infiltration analysis in IBC, the low IL-17 score group exhibited significantly higher infiltration fractions of most immune cells in luminal breast cancer. In HER2-enhanced breast cancer (*Figure 7D*), patients with low IL-17 scores showed higher immune infiltration levels of aDC, B cells, cytotoxic cells, DC, NK CD56bright cells, and T cells, while no significant difference was observed in the immune

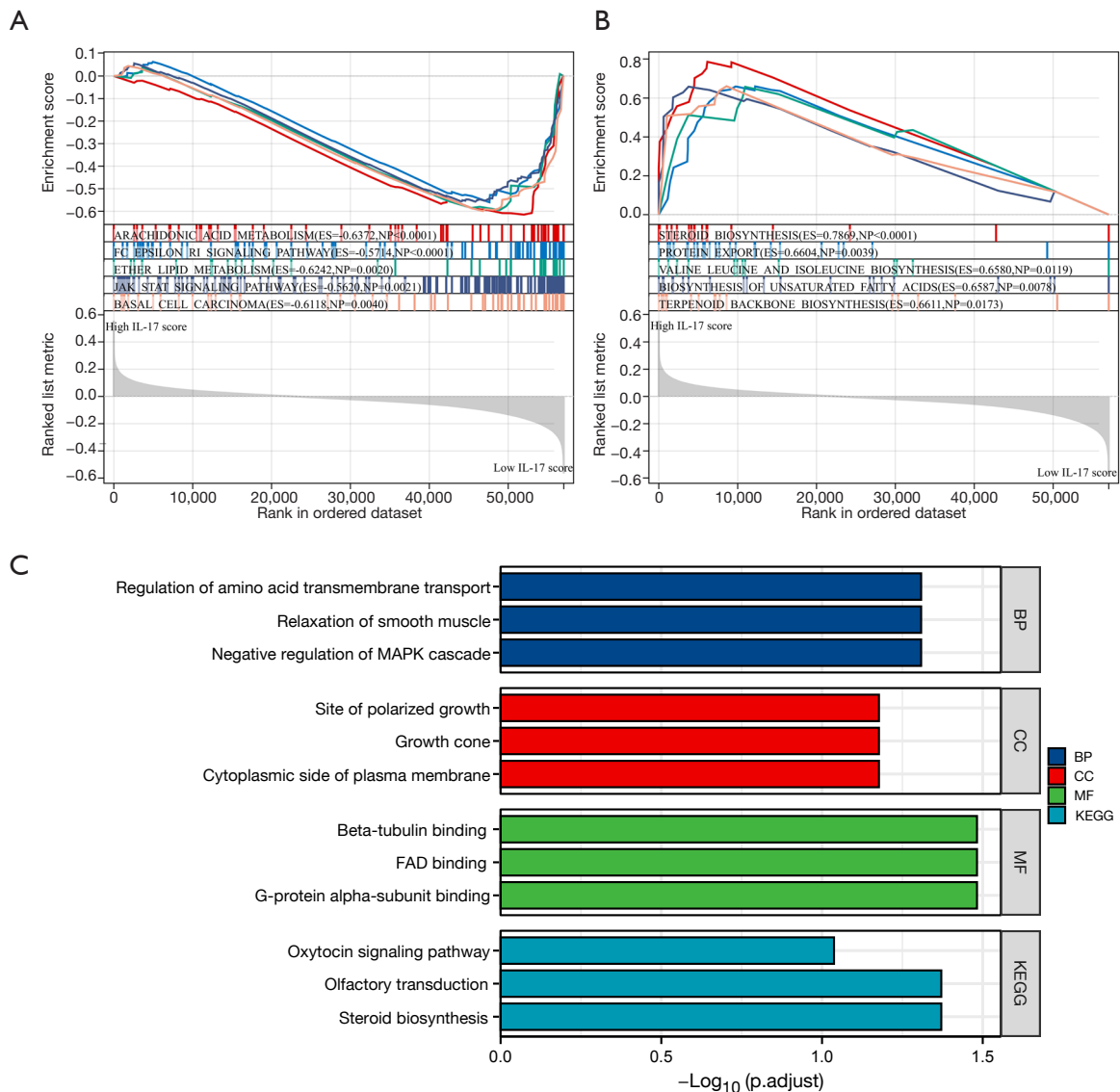


Figure 6 Functional enrichment analysis. (A) Top 5 differential pathway enriched in low IL-17 score group. (B) Top 5 differential pathway enriched in high IL-17 score group. (C) The GO and KEGG enrichment results of the 5 IL-17-related core prognostic genes. IL-17, interleukin 17; BP, biological process; CC, cell component; MF, molecular function; KEGG, Kyoto Encyclopedia of Genes and Genomes; GO, Gene Ontology; FAD, flavin adenine dinucleotide.

infiltration levels of other immune cells between the low and high IL-17 score groups. In the case of TNBC (Figure 7D), patients with low IL-17 scores had higher infiltration levels of CD8 T cells compared to those with high IL-17 scores ($P<0.05$), whereas Th17 cells and Th2 cells exhibited higher infiltration levels in patients with high IL-17 scores compared to those with low IL-17 scores. These findings indicate that the IL-17 score exerts a specific influence on immune infiltration in diverse subtypes of breast cancer.

Immunotherapy response

Recently, immunotherapy and targeted therapy have played important roles in clinical therapy for breast cancer and have become popular research topics. Therefore, 43 immune checkpoint candidate genes between the low and high IL-17 score groups were compared to determine the differences in response to immune-targeted therapy. As classical immune checkpoint genes, cytotoxic T-lymphocyte-associated protein 4 (CTLA4) and

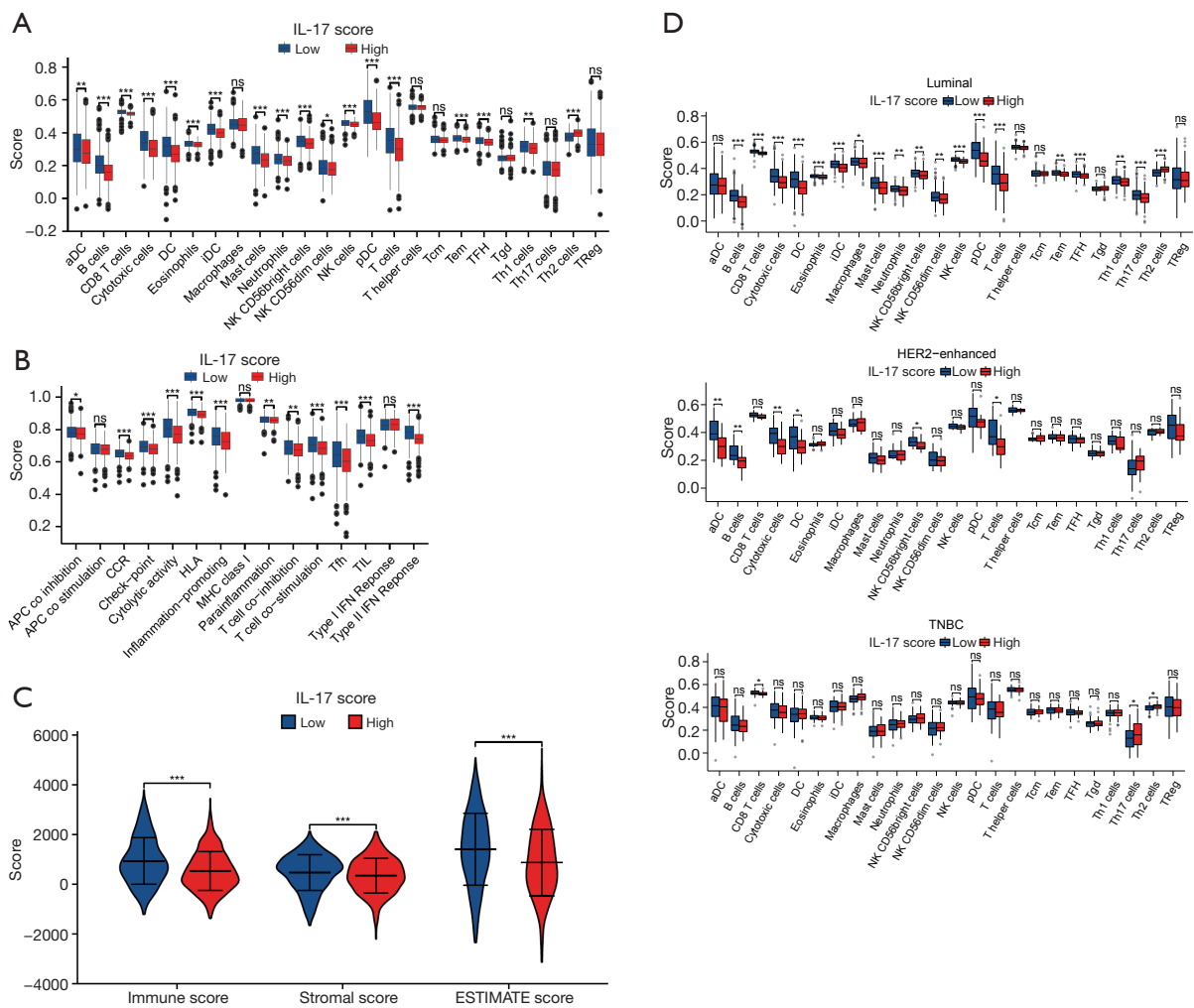


Figure 7 Comparison of tumor microenvironment immune infiltration characteristics between low and high IL-17 score groups. (A) Immune cell infiltration comparison between low and high IL-17 score groups. (B) Immune-related pathway enrichment comparison between the two groups. (C) Immune, stromal, and estimate score comparison between low and high IL-17 score groups. (D) Immune infiltration analysis of IL-17 score in breast cancer subtypes. Statistical significance symbols, ns, $P \geq 0.05$; *, $P < 0.05$; **, $P < 0.01$; ***, $P < 0.001$. IL-17, interleukin 17; NK, natural killer; TFH, T follicular helper cell; APC, antigen-presenting cell; CCR, C-C chemokine receptor; HLA, human leukocyte antigen; MHC, major histocompatibility complex; TIL, tumor-infiltrating lymphocyte; TNBC, triple-negative breast cancer; HER2, human epidermal growth factor receptor 2.

programmed cell death protein 1 (PD-1) were expressed at higher levels in the low IL-17 score group. Interestingly, 37 of the 43 immune checkpoint candidate genes were expressed at higher levels in the low IL-17 score group while only *TNFSF* had a lower expression in the low IL-17 score group. Therefore, patients in the low IL-17 score group were more likely to have enhanced responses to most checkpoint targeted therapies (Figure 8A). Immunogenomic analyses from TCIA indicated that patients with low IL-

17 scores had better predicted immunotherapy responses than those with high IL-17 scores. This trend was observed for CLTA4-targeted therapy, PD-1-targeted therapy, their combination, and therapies excluding PD-1 and CLTA4 (Figure 8B).

Chemotherapy sensitivity

As chemotherapy plays an important role pre- and post-

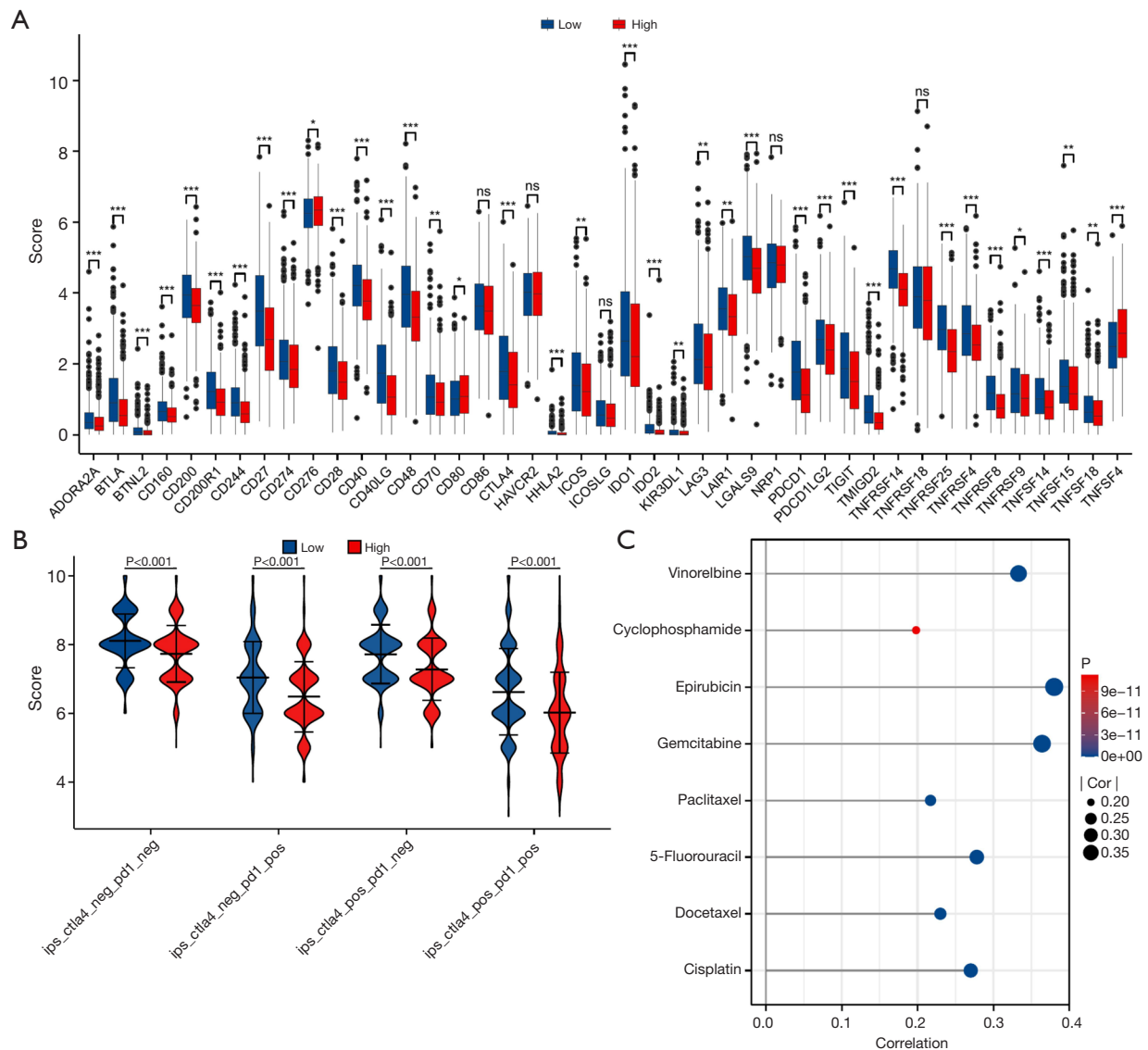


Figure 8 The results of chemotherapy sensitivity analysis and immunotherapy response analysis. (A) Comparison of 43 checkpoints expression between low and high IL-17 score groups. (B) Comparison of immunotherapy response of CTLA4 and PD-1 between low and high IL-17 score groups. (C) Correlation between the IC₅₀ of common chemotherapy drug for breast cancer and IL-17 score. Statistical significance symbols, ns, $P \geq 0.05$; *, $P < 0.05$; **, $P < 0.01$; ***, $P < 0.001$. IL-17, interleukin 17; CTLA4, cytotoxic T-lymphocyte-associated protein 4; PD-1, programmed cell death protein 1; IC₅₀, half maximal inhibitory concentration.

surgery in breast cancer patients, the role of the IL-17 score in chemotherapy for IBC patients was explored in this study. *Figure 8C* shows the correlation between IL-17 scores and the half maximal inhibitory concentration (IC₅₀) of common breast cancer chemotherapeutics. The IC₅₀ values of all drugs, including vinorelbine ($r=0.33$; $P < 0.001$),

cyclophosphamide ($r=0.20$; $P < 0.001$), epirubicin ($r=0.38$; $P < 0.001$), gemcitabine ($r=0.364$; $P < 0.001$), paclitaxel ($r=0.22$; $P < 0.001$), 5-fluorouracil ($r=0.28$; $P < 0.001$), docetaxel ($r=0.23$; $P < 0.001$), and cisplatin ($r=0.27$; $P < 0.001$), were positively correlated with the IL-17 score. These findings suggest that IL-17 scores may had a correlation with chemotherapy.

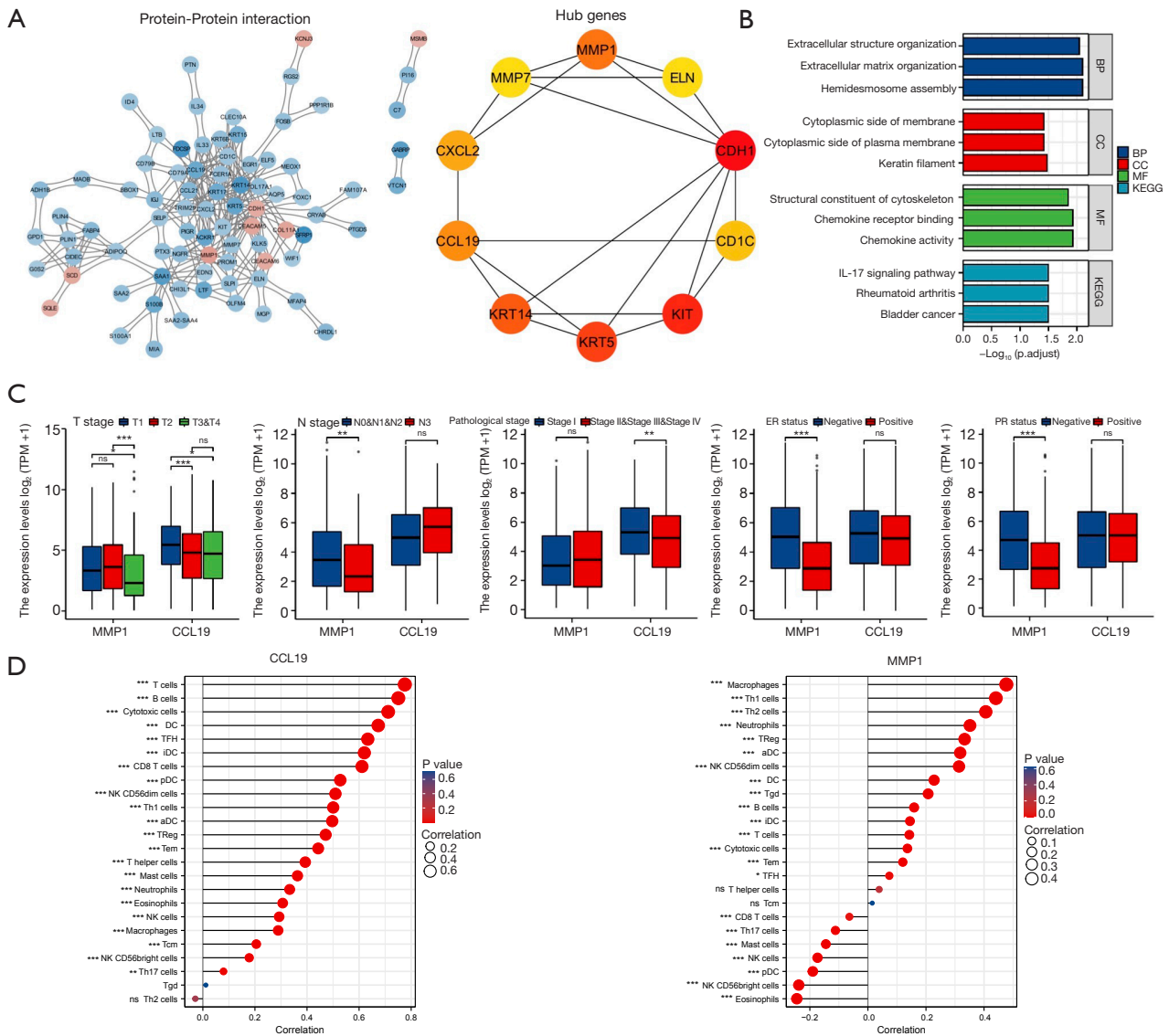


Figure 9 Protein interaction analysis and identification of hub genes. (A) PPI network and top ten hub genes. Blue, low expression DEGs in high IL-17 score group; red, high expression DEGs in high IL-17 score group. (B) The GO and KEGG analysis results of top ten hub genes. (C) The relationship between *MMP1* and *CCL19* expression level and clinicopathological characteristics. (D) Immune infiltration analysis of *MMP1* and *CCL19*. Statistical significance symbols, ns, $P \geq 0.05$; *, $P < 0.05$; **, $P < 0.01$; ***, $P < 0.001$. BP, biological process; CC, cell component; MF, molecular function; KEGG, Kyoto Encyclopedia of Genes and Genomes; TPM, transcripts per million; ER, estrogen receptor; PR, progesterone receptor; TFH, T follicular helper cell; NK, natural killer; PPI, protein-protein network; DEGs, differential expression genes; IL-17, interleukin 17; GO, Gene Ontology.

Construction of the PPI network and identification of hub genes based on the IL-17 score

Based on the DEGs between the low and high IL-17 score groups, a PPI network was constructed to further assess the core genes related to IL-17 (Figure 9A). A total of ten

hub genes were confirmed, including *CDH1*, *KIT*, *KRT5*, *KRT14*, *MMP1*, *CCL19*, *CXCL2*, *CD1C*, *MMP7*, and *ELN* (Figure 9A). GO and KEGG enrichment analyses were also performed to investigate the related biological functions and pathways. As shown in Figure 9B, the IL-17 signaling pathway was identified via KEGG analysis, which

Table 4 Results of univariate and multivariate Cox analysis of the ten hub genes

Gene	Univariate analysis		Multivariate analysis		
	Hazard ratio (95% CI)	P value	Coefficient	Hazard ratio (95% CI)	P value
<i>CDH1</i>	0.859 (0.612–1.206)	0.38	–	–	–
<i>KIT</i>	0.949 (0.861–1.046)	0.29	–	–	–
<i>ELN</i>	0.970 (0.886–1.061)	0.50	–	–	–
<i>KRT5</i>	0.924 (0.873–0.978)	0.007	–0.04	0.959 (0.851–1.081)	0.49
<i>KRT14</i>	0.932 (0.881–0.986)	0.01	0.004	1.004 (0.903–1.117)	0.93
<i>MMP1</i>	1.089 (1.017–1.166)	0.02	0.09	1.092 (1.015–1.175)	0.02
<i>CCL19</i>	0.893 (0.837–0.953)	<0.001	–0.11	0.899 (0.810–0.997)	0.04
<i>CXCL2</i>	0.862 (0.761–0.976)	0.02	–0.04	0.964 (0.827–1.123)	0.64
<i>CD1C</i>	0.861 (0.758–0.977)	0.02	0.07	1.071 (0.875–1.312)	0.51
<i>MMP7</i>	0.930 (0.866–0.998)	0.04	–0.02	0.979 (0.890–1.078)	0.67

CI, confidence interval.

also demonstrated the significant connection between the ten hub genes and IL-17. The other significant biological functions and pathways were hemidesmosome assembly, extracellular matrix, organization, extracellular structure organization, keratin filament, cytoplasmic side of plasma membrane, cytoplasmic side of membrane, chemokine activity, chemokine, receptor binding, structural constituent of cytoskeleton, bladder cancer, and rheumatoid arthritis. Furthermore, univariate and multivariate COX regression analyses were performed to explore the relationship between the hub genes and prognosis of patients with IBC. As shown in *Table 4*, *KRT5* [HR =0.92 (95% CI: 0.87–0.98); P=0.007], *KRT14* [HR =0.93 (95% CI: 0.88–0.99); P=0.01], *MMP1* [HR =1.09 (95% CI: 1.02–1.17); P=0.02], *CCL19* [HR =0.89 (95% CI: 0.84–0.95); P<0.001], *CXCL2* [HR =0.86 (95% CI: 0.76–0.98); P=0.02], *CD1C* [HR =0.86 (95% CI: 0.76–0.98); P=0.02], and *MMP7* [HR =0.93 (95% CI: 0.87–1.00); P=0.04] were identified as prognostic genes using univariate COX regression. *MMP1* [HR =1.09 (95% CI: 1.02–1.18); P=0.02] and *CCL19* [HR =0.90 (95% CI: 0.81–1.00); P=0.04] were identified as independent prognostic genes by multivariate COX regression, while *MMP1* was identified as a risk factor and *CCL19* was identified as a protective factor in patients with IBC. The two hub genes with independent prognostic relevance were explored to determine their relationship with clinical features. *Figure 9C* illustrates that the expression level of *MMP1* was significantly related to the T stage, N stage, estrogen receptor (ER) status, and

progesterone receptor (PR) status, while the expression level of *CCL19* was only related to T stage and pathological stage. Regarding the immune infiltration analysis, Th17 cells were found to be significantly negatively correlated with *MMP1* expression (*Figure 9D*), while the correlation between Th17 cells and *CCL19* was completely opposite (*Figure 9D*). These results of the immune analysis indicate that *MMP1* may be linked to the prognosis of patients with IBC.

Validation of mRNA and protein expression levels of IL-17-related core prognostic genes

The qRT-PCR analysis revealed the mRNA expression levels of *OR51E1*, *NDRG2*, *RGS2* and *TSPAN7* were found to be downregulated in breast tumor tissues compared to normal breast tissues (*Figure 10A*). However, no significant difference was observed in the mRNA expression levels of *SQLE* between the tumor and normal clinical samples (*Figure 10A*). To further explore the expression of IL-17-related core prognostic genes at the histological level, immunohistochemical staining of normal breast and tumor tissues was performed. As shown in *Figure 10B*, the expression levels of *OR51E1* and *NDRG2* in the breast tumor tissue were lower than those in the normal breast tissue, whereas the opposite was found for *SQLE*. There was no positive staining for *TSPAN7* in breast tumor tissues and normal breast tissues.

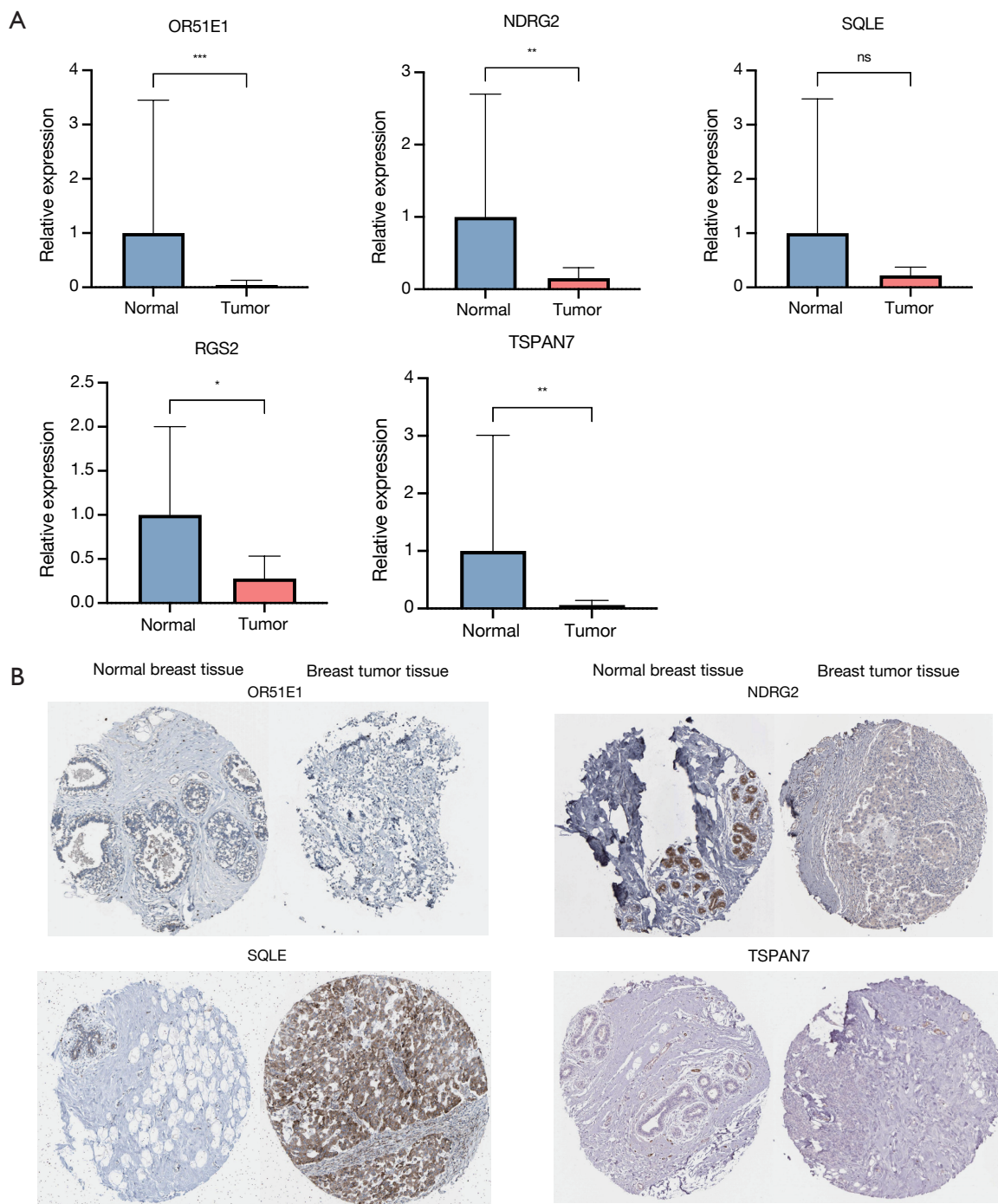


Figure 10 Validation of mRNA and protein expression levels of IL-17-related core prognostic genes. (A) The qRT-PCR results of mRNA expression levels of *OR51E1*, *NDRG2*, *SQLE*, *RGS2*, and *TSPAN7*. (B) Representative immunohistochemical staining for *OR51E1* (<https://www.proteinatlas.org/ENSG00000180785-OR51E1/cancer/breast+cancer>), *NDRG2* (<https://www.proteinatlas.org/ENSG00000211455-STK38L/cancer/breast+cancer>), *SQLE* (<https://www.proteinatlas.org/ENSG00000104549-SQLE/cancer/breast+cancer>), *TSPAN7* (<https://www.proteinatlas.org/ENSG00000156298-TSPAN7/cancer/breast+cancer>) in normal breast tissue and breast tumor tissue. Images were sourced from the Human Protein Atlas database (<https://www.proteinatlas.org/>). Statistical significance symbols, ns, $P \geq 0.05$; *, $P < 0.05$; **, $P < 0.01$; ***, $P < 0.001$. IL-17, interleukin 17; qRT-PCR, quantitative reverse transcription polymerase chain reaction.

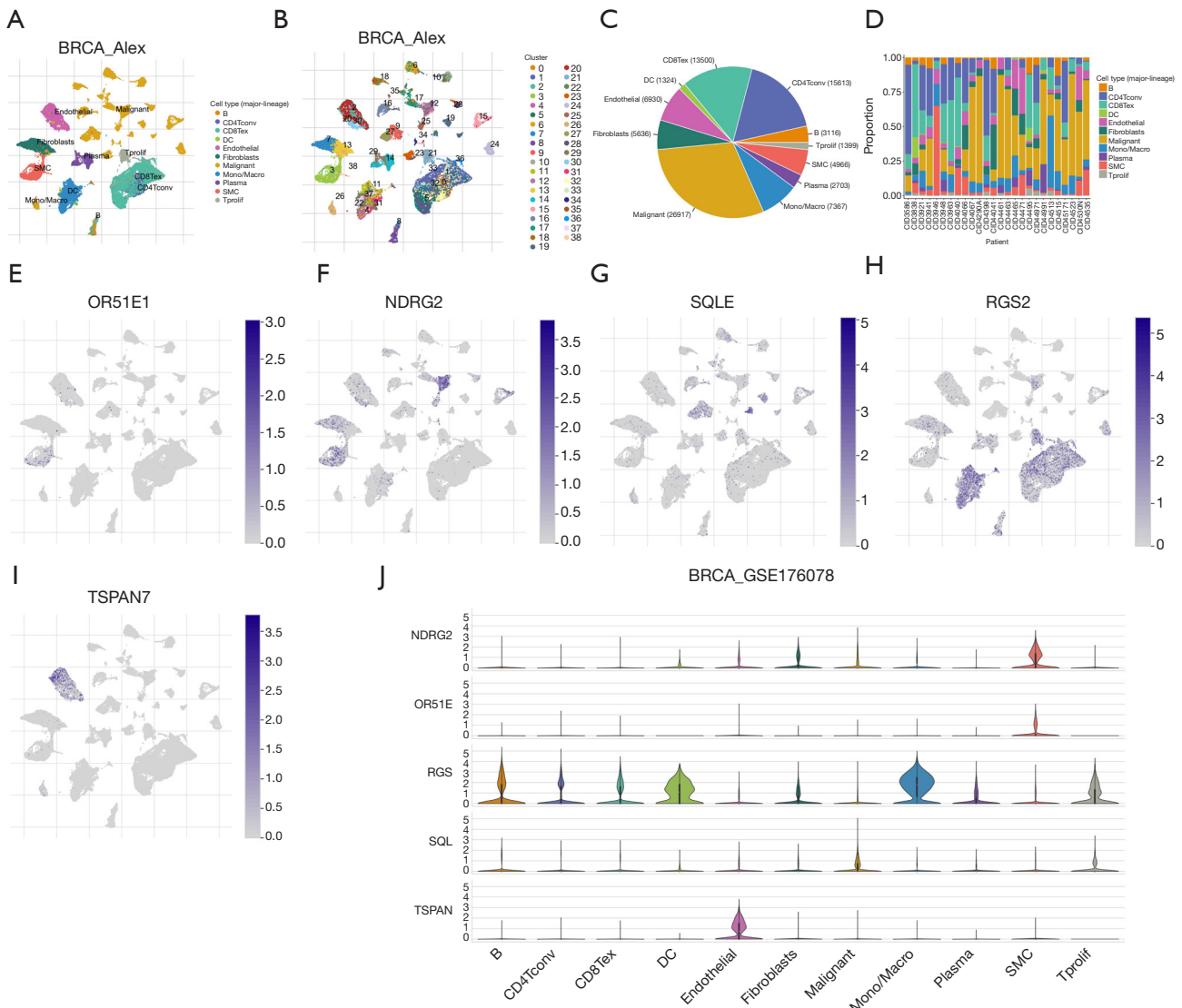


Figure 11 Five IL-17-related core genes expression in the immune infiltration characteristics of the TME-associated cells in IBC. (A-D) Annotation of all cell types in GSE176078 and the percentage of each cell type. (E-J) Expression of five IL-17-related core genes in TME-associated cells. BRCA, breast invasive carcinoma; SMC, smooth muscle cell; IL-17, interleukin 17; TME, tumor microenvironment; IBC, invasive breast cancer.

Correlation between IL-17-related core prognostic genes and TME based on single cell analysis

The single-cell dataset BRCA GSE176078 from the TISCH database was used to analyze the expression of five IL-17-related core genes in the immunological microenvironment. The dataset contains 39 cell populations and 11 cell types (Figure 11A,11B), with the distribution

and abundance of these types shown in Figure 11C,11D. Figure 11E-11J illustrate the expression levels of the five genes across various cell types. NDRG2, RGS2, and SQLE were detected in 11 cell types, including B cells, CD4Tcov, CD8Tex, DC, endothelial cells, fibroblasts, malignant cells, mono/macro, plasma cells, smooth muscle cell (SMC), and Tprolif. OR51E1 was primarily expressed in SMC, while TSPAN7 was mainly found in endothelial cells.

Discussion

Based on increasing research, IL-17 is a key factor in the development of IBC (33). The effect of IL-17 on breast cancer can be divided into two categories: direct and indirect. The direct effects of IL-17 on cancer cells include facilitating angiogenesis, altering gene expression profiles, and increasing invasiveness and tumor development *in vivo* (34). IL-17 depends on neutrophils to stimulate the development of metastatic primary breast cancer; hence, its effect is indirect (35). Some substances released by neutrophils regulate the destruction of the extracellular matrix and cell invasion, whereas IL-17 governs the recruitment of neutrophils, thereby producing an environment favorable for disease development. Through the ERK1/2 pathway, IL-17 produced by tumor-infiltrating lymphocytes (TILs) promotes the progression and drug resistance of breast cancer cells (36). However, most studies have focused on the mechanisms by which IL-17 regulates breast cancer development. The prognostic value and immune microenvironment in IBC based on IL-17-related signatures remain unclear.

To our knowledge, this is the first study to determine the significance of IL-17-related genes in the immune microenvironment and their prognostic value in IBC patients. Using bioinformatics analysis, this study revealed that the IL-17-related signatures were linked to the prognosis of IBC. In addition, the role of these signatures in the immune microenvironment and prognostic value for IBC patients were elucidated using survival analysis, immune cell infiltration, chemotherapy sensitivity, and immunotherapy response. Our findings may provide insights into the role of IL-17 in IBC progression and thus contribute to the establishment of an effective treatment plan.

Most of the IL-17-related core prognostic genes were found to be involved in the development of cancer. Based on previous studies, four of the five IL-17-related core prognostic genes (*NDRG2*, *SQLE*, *RGS2*, and *TSPAN7*) were associated with the development of breast cancer (37-40). N-myc downstream-regulated gene (*NDRG*) 2, a crucial member of the *NDRG* family, functions as a differentiation- and stress-related molecular regulator (41,42). Numerous forms of human malignancies, including breast cancer, downregulate *NDRG2* levels as tumor suppressors (43). Recently, *MiR-181a-5p* was demonstrated to help promote the proliferation, invasion, and glycolysis of breast cancer cells via the *NDRG2*-mediated activation

of the PTEN/AKT pathway (44). However, the function of *NDRG2* as an IL-17-related core prognostic gene in IBC remains unclear. In this study, *NDRG2* was incorporated into a predictive model based on IL-17 score to determine its corresponding role.

SQLE is a rate-limiting enzyme in cholesterol synthesis. A previous study has shown that *SQLE*, an important regulatory factor of iron death, has a significant impact on the development, immune microenvironment, and prognosis of breast cancer (39). *RGS2* is a G-protein coupled receptor regulator that encodes the regulator of G-protein signaling 2. *RGS2* was found to be differentially expressed in mammary epithelial subpopulations, overexpressed in most breast cancers (45), and mediates *miR-183-5p* to aggravate breast cancer (38). *TSPAN7*, or tetraspanin 7, is a conserved membrane protein found in the tetraspanin protein superfamily (46) and has been reported to be associated with the prediction of breast cancer survival as a tumor-associated high endothelial venules-upregulated gene (37). In summary, the above studies indicate that *NDRG2*, *SQLE*, *RGS2*, and *TSPAN7* are related to the prognosis of breast cancer patients. Herein, these conclusions were verified through an evaluation of the significance of these genes in a prognostic model based on IL-17-related signatures.

In this investigation, it was observed that *OR51E1*, *NDRG2*, *RGS2*, and *TSPAN7* exhibited decreased expression in breast tumor tissues in comparison to normal breast tissues at the RNA level. This finding was authenticated by qRT-PCR analysis. Additionally, the protein expression levels of *OR51E1*, *NDRG2*, and *SQLE* in normal breast tissue and tumor tissue were confirmed via immunohistochemical assays. Notably, Wang *et al.* (47) reported that *RGS2* had reduced expression in breast tumor tissue compared to normal breast tissue based on immunohistochemical experiments, thus validating the expression of *RGS2* at the protein level. On the other hand, *TSPAN7* did not demonstrate any positive staining in either breast tumor tissues or normal breast tissues. This is likely due to the high expression of *TSPAN7* in the endothelial cells of tertiary lymphoid structure-associated blood vessels, while minimal or no expression was noted in cancer cells or other stromal cells in breast cancer (37).

IL-17 is a crucial factor associated with IBC progression. In this study, a high IL-17 score was linked to adverse outcomes and malignant development in patients with IBC. For instance, age was positively correlated with the IL-17 score, and IBC patients with T4 had the highest IL-

17 score. However, patients with N3 had the lowest IL-17 score; this may be because the increase in neutrophils in breast cancer can promote lymphatic metastasis of tumor cells (35), and patients with lower IL-17 scores had a higher neutrophil infiltration level. Interestingly, the IL-17 score was observed to be highest in HER2-enriched breast cancer and lowest in TNBC. This observation can largely be attributed to the prognostic model based on the IL-17 score, in which *OR51E1*, acting as a risk factor, demonstrates the highest risk coefficient among other prognostic genes. Moreover, the expression of *OR51E1* in TNBC significantly undercuts that in HER2-enriched breast cancer. This finding underscores the potential of *OR51E1* as a promising marker for elucidating disparities among various breast cancer subtypes in future research.

In this research, the prognostic model developed using the IL-17 score can be used to predict the OS of patients with IBC. Using this prognostic model, patients with low IL-17 scores were found to have a better OS than those with high IL-17 scores in TCGA, as confirmed by verifying the IBC data from METABRIC. This finding indicates that this prognostic model can perform well when used to identify IBC populations with better or worse OS. Additionally, the combination of clinicopathological factors linked to prognosis and the prognostic model based on the IL-17 score boosted the model's predictive power and clinical usefulness.

To gain a better understanding of the role of the prognostic model based on the IL-17 score in IBC, we investigated the relationship between chemotherapy and the IL-17 score. Vinorelbine, cyclophosphamide, epirubicin, gemcitabine, paclitaxel, 5-fluorouracil, docetaxel, and cisplatin are commonly used drugs for breast cancer chemotherapy. We found a negative correlation between the IC_{50} values of these drugs and the IL-17 score, indicating a strong association between the IL-17 score and chemotherapy. However, it is important to note that this correlation does not imply causality, and it remains uncertain whether IL-17 signaling directly affects drug sensitivity. Further experimental and clinical studies are needed to establish whether there is a causal relationship and to explore how these findings might translate into clinical practice. This finding nonetheless supports the potential of the prognostic model and suggests future possibilities for combining targeted therapy with chemotherapy in the treatment of IBC.

Recently, TME has been considered an important part

of the development, progression, and response to therapy in breast cancer (48). According to a previous study, CD8 T cell infiltration in the breast TME is associated with longer breast cancer survival, which was also observed in this study (49). Herein, individuals with low IL-17 scores had a higher CD8 T cell infiltration fraction and a significantly longer OS than patients with high IL-17 scores. The infiltration levels of neutrophils were found to significantly differ between patients with high and low IL-17 scores, and IL-17 was found to create an immunosuppressive environment by controlling neutrophil recruitment to promote tumor progression (33), suggesting that neutrophils may be crucial immune cells mediating immunosuppression in the high IL-17 TME. The interplay between IL-17 and the breast cancer TME could be leveraged to develop novel immunotherapy regimens (50).

In this study, a strong correlation was found between the IL-17 score and immune cell infiltration in patients with IBC. This finding indicates that the IL-17 score holds potential as a target for future immunotherapy approaches, aimed at improving the prognosis of IBC patients. These results have promising implications for the development of personalized immunotherapy strategies and the enhancement of treatment outcomes.

There are some limitations in this study. While the IL-17-related signature shows potential as a prognostic marker in IBC, its underlying molecular mechanisms remain unclear. Future studies are needed to experimentally investigate these mechanisms to confirm the specific role of IL-17 signaling in tumor progression and immune regulation. Additionally, we plan to develop cell and animal models to further validate our findings and enhance our understanding of the IL-17 pathway's contribution to IBC prognosis.

Conclusions

This study sought to assess the prognostic value and immune microenvironment of the IL-17-related signatures in IBC. Based on the clinicopathological characteristics and IL-17 scores, the nomogram can be utilized to predict the OS of patients with IBC in clinical setting. The correlation between IL-17 scores and chemotherapy or immunotherapy of IBC patients was found to be highly significant. Furthermore, IL-17 score was significantly linked to immune component infiltration, which might be useful in the development of innovative targeted therapies and immunotherapy. IL-17-related signatures can be used

as prognostic biomarkers for patients with IBC. These findings may lay a foundation for future individualized IBC therapies.

Acknowledgments

None.

Footnote

Reporting Checklist: The authors have completed the TRIPOD reporting checklist. Available at <https://tcr.amegroups.com/article/view/10.21037/tcr-24-1632/rc>

Peer Review File: Available at <https://tcr.amegroups.com/article/view/10.21037/tcr-24-1632/prf>

Funding: This work was supported by the Natural Science Foundation of Shanghai, China (No. 21ZR1451000) and the Shanghai Municipal Health Commission, China (No. 20214Y0255).

Conflicts of Interest: All authors have completed the ICMJE uniform disclosure form (available at <https://tcr.amegroups.com/article/view/10.21037/tcr-24-1632/coif>). The authors have no conflicts of interest to declare.

Ethical Statement: The authors are accountable for all aspects of the work in ensuring that questions related to the accuracy or integrity of any part of the work are appropriately investigated and resolved. The study was conducted in accordance with the Declaration of Helsinki (as revised in 2013).

Open Access Statement: This is an Open Access article distributed in accordance with the Creative Commons Attribution-NonCommercial-NoDerivs 4.0 International License (CC BY-NC-ND 4.0), which permits the non-commercial replication and distribution of the article with the strict proviso that no changes or edits are made and the original work is properly cited (including links to both the formal publication through the relevant DOI and the license). See: <https://creativecommons.org/licenses/by-nc-nd/4.0/>.

References

- Loibl S, Poortmans P, Morrow M, et al. Breast cancer. *Lancet* 2021;397:1750-69.
- Siegel RL, Giaquinto AN, Jemal A. Cancer statistics, 2024. *CA Cancer J Clin* 2024;74:12-49.
- Waks AG, Winer EP. Breast Cancer Treatment. *JAMA* 2019;321:316.
- Cua DJ, Tato CM. Innate IL-17-producing cells: the sentinels of the immune system. *Nat Rev Immunol* 2010;10:479-89.
- Le Gouvello S, Bastuji-Garin S, Aloulou N, et al. High prevalence of Foxp3 and IL17 in MMR-proficient colorectal carcinomas. *Gut* 2008;57:772-9.
- Miyahara Y, Odunsi K, Chen W, et al. Generation and regulation of human CD4+ IL-17-producing T cells in ovarian cancer. *Proc Natl Acad Sci U S A* 2008;105:15505-10.
- Lv Z, Liu M, Shen J, et al. Association of serum interleukin-10, interleukin-17A and transforming growth factor- α levels with human benign and malignant breast diseases. *Exp Ther Med* 2018;15:5475-80.
- Fukui Y, Kawashima M, Kawaguchi K, et al. Granulocyte-colony-stimulating factor-producing metaplastic carcinoma of the breast with significant elevation of serum interleukin-17 and vascular endothelial growth factor levels. *Int Cancer Conf J* 2018;7:107-13.
- Wu L, Awaji M, Saxena S, et al. IL-17-CXC Chemokine Receptor 2 Axis Facilitates Breast Cancer Progression by Up-Regulating Neutrophil Recruitment. *Am J Pathol* 2020;190:222-33.
- Qian XL, Xu P, Zhang YQ, et al. Increased number of intratumoral IL-17+ cells, a harbinger of the adverse prognosis of triple-negative breast cancer. *Breast Cancer Res Treat* 2020;180:311-9.
- Tsai YF, Huang CC, Lin YS, et al. Interleukin 17A promotes cell migration, enhances anoikis resistance, and creates a microenvironment suitable for triple negative breast cancer tumor metastasis. *Cancer Immunol Immunother* 2021;70:2339-51.
- Chen WC, Lai YH, Chen HY, et al. Interleukin-17-producing cell infiltration in the breast cancer tumour microenvironment is a poor prognostic factor. *Histopathology* 2013;63:225-33.
- Zhao J, Chen X, Herjan T, et al. The role of interleukin-17 in tumor development and progression. *J Exp Med* 2020;217:e20190297.
- Clarke C, Madden SF, Doolan P, et al. Correlating transcriptional networks to breast cancer survival: a large-scale coexpression analysis. *Carcinogenesis* 2013;34:2300-8.
- Curtis C, Shah SP, Chin SF, et al. The genomic and

- transcriptomic architecture of 2,000 breast tumours reveals novel subgroups. *Nature* 2012;486:346-52.
16. Love MI, Huber W, Anders S. Moderated estimation of fold change and dispersion for RNA-seq data with DESeq2. *Genome Biol* 2014;15:550.
 17. Barrett T, Wilhite SE, Ledoux P, et al. NCBI GEO: archive for functional genomics data sets--update. *Nucleic Acids Res* 2013;41:D991-5.
 18. Liu J, Lichtenberg T, Hoadley KA, et al. An Integrated TCGA Pan-Cancer Clinical Data Resource to Drive High-Quality Survival Outcome Analytics. *Cell* 2018;173:400-416.e11.
 19. Engebretsen S, Bohlin J. Statistical predictions with glmnet. *Clin Epigenetics* 2019;11:123.
 20. Gao J, Aksoy BA, Dogrusoz U, et al. Integrative analysis of complex cancer genomics and clinical profiles using the cBioPortal. *Sci Signal* 2013;6:pl1.
 21. Ringnér M. What is principal component analysis? *Nat Biotechnol* 2008;26:303-4.
 22. Van Calster B, Wynants L, Verbeek JFM, et al. Reporting and Interpreting Decision Curve Analysis: A Guide for Investigators. *Eur Urol* 2018;74:796-804.
 23. Yu G, Wang LG, Han Y, et al. clusterProfiler: an R package for comparing biological themes among gene clusters. *OMICS* 2012;16:284-7.
 24. Hänzelmann S, Castelo R, Guinney J. GSEA: gene set variation analysis for microarray and RNA-seq data. *BMC Bioinformatics* 2013;14:7.
 25. Bindea G, Mlecnik B, Tosolini M, et al. Spatiotemporal dynamics of intratumoral immune cells reveal the immune landscape in human cancer. *Immunity* 2013;39:782-95.
 26. Yoshihara K, Shahmoradgoli M, Martínez E, et al. Inferring tumour purity and stromal and immune cell admixture from expression data. *Nat Commun* 2013;4:2612.
 27. Charoentong P, Finotello F, Angelova M, et al. Pan-cancer Immunogenomic Analyses Reveal Genotype-Immunophenotype Relationships and Predictors of Response to Checkpoint Blockade. *Cell Rep* 2017;18:248-62.
 28. Maeser D, Gruener RF, Huang RS. oncoPredict: an R package for predicting in vivo or cancer patient drug response and biomarkers from cell line screening data. *Brief Bioinform* 2021;22:bbab260.
 29. Ritchie ME, Phipson B, Wu D, et al. limma powers differential expression analyses for RNA-sequencing and microarray studies. *Nucleic Acids Res* 2015;43:e47.
 30. Szklarczyk D, Gable AL, Lyon D, et al. STRING v11: protein-protein association networks with increased coverage, supporting functional discovery in genome-wide experimental datasets. *Nucleic Acids Res* 2019;47:D607-13.
 31. Shannon P, Markiel A, Ozier O, et al. Cytoscape: a software environment for integrated models of biomolecular interaction networks. *Genome Res* 2003;13:2498-504.
 32. Chin CH, Chen SH, Wu HH, et al. cytoHubba: identifying hub objects and sub-networks from complex interactome. *BMC Syst Biol* 2014;8 Suppl 4:S11.
 33. Song X, Wei C, Li X. The potential role and status of IL-17 family cytokines in breast cancer. *Int Immunopharmacol* 2021;95:107544.
 34. Benevides L, da Fonseca DM, Donate PB, et al. IL17 Promotes Mammary Tumor Progression by Changing the Behavior of Tumor Cells and Eliciting Tumorigenic Neutrophils Recruitment. *Cancer Res* 2015;75:3788-99.
 35. Coffelt SB, Kersten K, Doornebal CW, et al. IL-17-producing $\gamma\delta$ T cells and neutrophils conspire to promote breast cancer metastasis. *Nature* 2015;522:345-8.
 36. Mombelli S, Cochaud S, Merrouche Y, et al. IL-17A and its homologs IL-25/IL-17E recruit the c-RAF/S6 kinase pathway and the generation of pro-oncogenic LMW-E in breast cancer cells. *Sci Rep* 2015;5:11874.
 37. Sawada J, Hiraoka N, Qi R, et al. Molecular Signature of Tumor-Associated High Endothelial Venules That Can Predict Breast Cancer Survival. *Cancer Immunol Res* 2022;10:468-81.
 38. Wu C, Tuo Y, Hu G, et al. miR-183-5p Aggravates Breast Cancer Development via Mediation of RGS2. *Comput Math Methods Med* 2021;2021:9664195.
 39. Tang W, Xu F, Zhao M, et al. Ferroptosis regulators, especially SQLE, play an important role in prognosis, progression and immune environment of breast cancer. *BMC Cancer* 2021;21:1160.
 40. Lee A, Lim S, Oh J, et al. NDRG2 Expression in Breast Cancer Cells Downregulates PD-L1 Expression and Restores T Cell Proliferation in Tumor-Coculture. *Cancers (Basel)* 2021;13:6112.
 41. Le TM, Takarada-Iemata M, Tà HM, et al. NdrG2 deficiency ameliorates neurodegeneration in experimental autoimmune encephalomyelitis. *J Neurochem* 2018;145:139-53.
 42. Hu W, Fan C, Jiang P, et al. Emerging role of N-myc downstream-regulated gene 2 (NDRG2) in cancer. *Oncotarget* 2016;7:209-23.
 43. Lorentzen A, Lewinsky RH, Bornholdt J, et al. Expression

- profile of the N-myc Downstream Regulated Gene 2 (NDRG2) in human cancers with focus on breast cancer. *BMC Cancer* 2011;11:14.
44. Zhai Z, Mu T, Zhao L, et al. MiR-181a-5p facilitates proliferation, invasion, and glycolysis of breast cancer through NDRG2-mediated activation of PTEN/AKT pathway. *Bioengineered* 2022;13:83-95.
45. Smalley MJ, Iravani M, Leao M, et al. Regulator of G-protein signalling 2 mRNA is differentially expressed in mammary epithelial subpopulations and over-expressed in the majority of breast cancers. *Breast Cancer Res* 2007;9:R85.
46. Yu X, Li S, Pang M, et al. TSPAN7 Exerts Anti-Tumor Effects in Bladder Cancer Through the PTEN/PI3K/AKT Pathway. *Front Oncol* 2020;10:613869.
47. Wang C, Ye Q, Cao Y, et al. Downregulation of regulator of G protein signaling 2 expression in breast invasive carcinoma of no special type: Clinicopathological associations and prognostic relevance. *Oncol Lett* 2018;15:213-20.
48. Mittal S, Brown NJ, Hoken I. The breast tumor microenvironment: role in cancer development, progression and response to therapy. *Expert Rev Mol Diagn* 2018;18:227-43.
49. Mahmoud SM, Paish EC, Powe DG, et al. Tumor-infiltrating CD8+ lymphocytes predict clinical outcome in breast cancer. *J Clin Oncol* 2011;29:1949-55.
50. Moaaz M, Lotfy H, Motawea MA, et al. The interplay of interleukin-17A and breast cancer tumor microenvironment as a novel immunotherapeutic approach to increase tumor immunogenicity. *Immunobiology* 2021;226:152068.

Cite this article as: Dong W, Gu X, Li J, Zhuang Z. Characterization of immune landscape and prognostic value of IL-17-related signature in invasive breast cancer. *Transl Cancer Res* 2025;14(2):907-929. doi: 10.21037/tcr-24-1632